

***np*-elastic analyzing power A_{N0} and spin transfer K_{NN}**

M. W. McNaughton, K. Johnston,* D. R. Swenson, D. Tupa, and R. L. York
Los Alamos National Laboratory, Los Alamos, New Mexico 87545

D. A. Ambrose, P. Coffey, K. H. McNaughton, and P. J. Riley
University of Texas, Austin, Texas 78712

G. Glass† and J. C. Hiebert
Texas A&M University, College Station, Texas 77843

R. H. Jeppesen
University of Montana, Missoula, Montana 59812

H. Spinka
Argonne National Laboratory, Argonne, Illinois 60439

Ivan Supek
Rudjer Boskovic Institute, Zagreb, Croatia

G. E. Tripard
Washington State University, Pullman, Washington 99164

H. Woolverton
University of Central Arkansas, Conway, Arkansas 72032
 (Received 9 February 1993)

We have measured the analyzing power A_{N0} and the spin transfer K_{NN} for *np*-elastic scattering from about 60° to 170° c.m. at 485, 635, and 788 MeV. The new data clarify previous discrepancies and complete the first-order determination of nucleon-nucleon elastic scattering at these energies.

I. INTRODUCTION

The primary goal of the nucleon-nucleon (*NN*) program at LAMPF is the complete determination of the phase shifts and amplitudes for *NN* elastic scattering up to 800 MeV. These are essential for microscopic models of the nucleus in addition to being a fundamental test of the strong interaction. Precise data such as the analyzing powers reported here are also important to calibrate other experimental facilities.

NN elastic scattering is described by five complex amplitudes for isospin 1 and five for isospin 0. The isospin-1 parameters have been determined by measuring more than ten spin-dependent *pp* observables [1,2] as a result of which the isospin-1 phase-shift analyses [3–6] are now well determined and in satisfactory agreement. The isospin-0 phase shifts [3–7] and amplitudes are determined from *np* scattering.

Allowing for some overdetermination it was agreed [8] that the following 11 *np* experimental parameters [9,10] should be measured over a wide angular range: cross section, analyzing power A_{N0} , the four spin correlation parameters A_{NN} , A_{SS} , A_{SL} , A_{LL} , and the five spin-transfer parameters K_{NN} , K_{SS} , K_{SL} , K_{LS} , K_{LL} .

It was also agreed [8] that an intense polarized ion source was essential for these measurements and consequently the Optically Pumped Polarized Ion Source (OPPIS) was built and completed in 1990. The OPPIS is essential for two reasons: (1) The high intensity is needed to provide adequate rates for triple scattering experiments; (2) the OPPIS lasers flip the spin without measurable side effects (Secs. III E 3 and III E 4).

The data reported here complete the planned set of measurements. The phase-shift analyses (PSA's) [3–7] are now relatively stable for both isospin 0 and isospin 1.

II. PREVIOUS DATA

The data are conveniently accessed via the SAID data base [3]. Observables are defined in Refs. [9,10] as well as in the papers that report the measurements. The *pp* data are discussed in Refs. [1,2] and further references therein. Previous *np* data in the range 485–800 MeV are summarized in this section.

*Present address: Louisiana Tech University, Ruston, Louisiana 71272.

†Present address: University of Texas, Austin, Texas 78712.

A. Cross-section data

Previous cross-section data include the total cross section σ , the total cross-section difference $\Delta\sigma_L(np)$ for longitudinally polarized n and p , and the differential cross section $d\sigma/d\Omega$.

The np total cross section was measured at LAMPF [11], the Princeton PPA [12], SIN-PSI [13], and TRIUMF [14]. The LAMPF and PPA data both claim uncertainties less than 1%, but they disagree by up to 5%. The TRIUMF data tend to agree with the PPA data and the PSI data tend to agree with LAMPF. The different PSA's handle this discrepancy in different ways, e.g., by omitting or renormalizing some data, resulting in discrepancies among the PSA's of a few percent.

The earliest $\Delta\sigma_L(np)$ data were deduced from measurements with a proton beam on a polarized-deuteron target [15]. These data have now been superseded by measurements with a free neutron beam on a polarized-proton target [16–18]. Arndt's PSA fails to reproduce the energy dependence, leading to speculation about a possible isospin-0 resonance [16]. Bugg's PSA, however, produces a satisfactory fit [4,7] to the data. Note that the recalibration of the LAMPF polarized-neutron beam [19] implies a renormalization of the $\Delta\sigma_L(np)$ data [16] of about 12% (Sec. IV).

There are several measurements of the np differential cross section from LAMPF [20–24], Saclay [25], and TRIUMF [14]. Typical uncertainties are a few percent and agreement with the PSA's is generally satisfactory.

B. Analyzing power

There are many measurements of the np analyzing power A_{N0} or A_{0N} . Compared with the best previous data, however, the present data have 10 times the statistical weight and are at least a factor of 3 better in systematic uncertainties.

At forward angles, most of the previous data were obtained by scattering a polarized-proton beam from the neutron in deuterium [26–31], except at the most forward angles where final-state interactions might distort these quasifree data and where free neutron data exist [32–34]. Near 800 MeV the Saclay forward-angle data [32,34] disagree with the LAMPF quasifree data [31]. Arndt *et al.* [3] and Bugg [4] renormalize these data, but the Saclay analysis [5] does not. Also note that the small statistical uncertainties in Refs. [28,29] were later revised to include systematic errors [3].

At backward angles, there are previous analyzing power data from TRIUMF [35,36], SATURNE [37], and LAMPF [38]. The older TRIUMF data [35] pass through zero at a different angle from the recent precise data [36]; Bugg [4] concludes that there was an error in the angle calibration and omits the older data [35]. Our present data support this conclusion (Sec. III E 9). Also, the data reported here disagree with the magnitude of the older LAMPF data [38]. This disagreement has been discussed before [4] and seems to be a normalization problem from the polarized target that was used previously.

C. Spin correlation

The same normalization problem [4] also extends to many of the spin correlation parameters measured at LAMPF [39,40] since these were normalized to the data of Ref. [38] (see Sec. IV). However, the Saclay A_{ZZ} data [41] do not support a renormalization.

D. Spin depolarization

At forward angles, there are spin-depolarization parameters measured by quasifree scattering of polarized protons from the neutron in deuterium, measuring the polarization of the scattered proton [42,43]. The disagreement with the PSA's at the most forward angles might be related to final-state interactions. The agreement of the spin-depolarization parameters between the pp and ${}^2\text{H}(p,p)np$ reactions does not necessarily imply agreement between np and ${}^2\text{H}(p,n)pp$ since the np and pp final state interactions are different.

E. Spin transfer

At backward angles, there are spin-transfer data measured with free neutrons on a liquid hydrogen target [44–47]. Agreement is satisfactory between the recent LAMPF data [46] and the older TRIUMF data near 500 MeV [44]. The present K_{NN} data near 500 MeV have 5 times the statistical weight of previous data [44]; agreement is satisfactory (Fig. 1). Near 650 MeV, the K_{NN} data from Berkeley are incorrect; on page 18 of Surko's thesis [48] Eq. 3.4 is incorrectly derived from Eq. 3.3 by changing the sign of P_1 in the numerator but not in the denominator. These data [48] are now omitted from most PSA's. Near 800 MeV, the present data extend the angular range of the previous data [47] (see Fig. 3).

F. Summary

In summary, there are extensive np -elastic data which are sufficient in principle to determine the phase shifts and amplitudes at several energies up to 800 MeV. After including the present data, the remaining disagreements among the phase-shift analyses are largely the result of (a) the renormalization or omission of some suspect data and (b) different choices on which partial waves should be allowed to contain inelasticity.

III. EXPERIMENTAL METHOD

A. Apparatus

The apparatus and experimental method used in the present measurements is essentially the same as was described previously [45,46]. Briefly, the polarized-neutron beam was obtained from the LAMPF polarized-proton beam striking a liquid deuterium target from which the neutrons were collimated at zero degrees [39,40]. All three components of the proton-beam polarization were measured [49]; the neutron-beam polarization was then obtained when each component was multiplied by the

appropriate spin-transfer coefficient [19] for the ${}^2\text{H}(p, n)$ reaction.

The polarized-neutron beam was collimated onto a 39-cm-thick by 24-cm-diam liquid hydrogen target. Recoil protons were detected in a magnetic spectrometer and their polarization was analyzed in the Janus [50] carbon polarimeter. Scattered neutrons were detected in a high-efficiency neutron detector [51].

The only differences between this and previous experiments [45,46] were as follows: A superconducting solenoid was added to precess the neutrons to N spin, i.e., normal to the scattering plane, and the vertical bend in the Scylla magnet was replaced by a horizontal bend in the Vartola magnet in order to avoid precession of the vertical proton spin.

B. Background

As in previous experiments [45,46], the background was measured both by interpolation under the momentum peak [see Fig. 2(a) of Ref. [45]] as well as by a comparison of the results obtained with and without the neutron detector [see Fig. 2(b) of Ref. [45]]. Both results were consistent with the calculated [46] background. The final corrections were 1% or less, with an uncertainty that was always negligible compared with counting statistics.

C. Spin-transfer K_{NN}

The np -elastic spin-transfer parameters K_{ij} give the polarization transfer from the incident neutrons to the recoil protons. The subscripts NN specify that the polarization of both particles is normal to the scattering plane (N spin).

The relevant equations and methods have been described previously [52]. In particular, it has been shown that, with suitable algebra, instrumental asymmetries cancel to first order when the beam spin is flipped from spin up (+) to down (-). If e_+ and e_- are the left-right asymmetries measured in the Janus [50] carbon polarimeter with + and - incident beam spins, then

$$K_{NN} = \frac{e_+ - e_-}{2A_C P} (1 - A_{N0}^2 P^2) + A_{N0}^2,$$

where A_{N0} is the analyzing power interpolated from the measurements described below. The 2% uncertainty in the carbon analyzing power A_C [53] has been included in the data in the tables as a point-to-point uncertainty, but is negligible compared with counting statistics. In addition, there is an overall normalization uncertainty arising from the calibration of the beam polarization P [19]. At 485 MeV, this is 2% and is common to all the data in Table III of Ref. [46] as well as all the data in Tables I and IV of this paper. At 635 MeV the 2% overall normalization uncertainty is common to Table II of Ref. [46] as well as Tables II and V of this paper. At 788 MeV the overall normalization uncertainty is 2.4% and is common to Table II of Ref. [45] as well as Tables III and VI of this paper.

D. Analyzing power A_{N0}

The scattering of a beam with polarization P normal to the scattering plane (N spin) is given by

$$\frac{N_+}{I_+} = \frac{d\sigma}{d\Omega} \Omega t (1 + AP),$$

where N_+ is the number of events scattered into a detector with solid angle Ω from a beam I_+ incident on a target with thickness t (nuclei/cm²), $d\sigma/d\Omega$ is the cross section (cm²), A is the analyzing power, and P is the beam polarization. If the beam spin is flipped, changing the sign of P , then

$$\frac{N_-}{I_-} = \frac{d\sigma}{d\Omega} \Omega t (1 - AP).$$

Defining $r = (N_+ I_-)/(N_- I_+)$, then A is given by

$$AP = \frac{r - 1}{r + 1}.$$

The selection of good events, N , has been described previously [45]. Briefly, good np -elastic events had the correct incident neutron time of flight, the correct scattered proton momentum and time of flight in the magnetic spectrometer, and a proton trajectory that originated in the liquid hydrogen target. The number of good events N was corrected for efficiency, live time, and background as discussed in Secs. III B and III E 5.

The basic techniques for measuring the beam polarization have also been described before. The x , y , and z components of the proton polarization were measured with the beam line polarimeters [49]. The x , y , and z components of the neutron polarization were then obtained by multiplying each component by the spin-transfer coefficients [19].

The calculated neutron-spin direction was compared with direct measurements. Previous measurements [45,46] agreed to better than 1°. During the present experiment this was reconfirmed with a statistical uncertainty of 2°, which corresponds to an uncertainty of $\Delta P/P = 1 - \cos(2^\circ) = 0.001$ for these N -spin data.

E. Systematic errors in A_{N0}

Section III D describes the basic equations for the analyzing power, but for precise measurements (typically with uncertainties of 0.01 or less) some underlying assumptions need to be examined. This section describes the second-order problems that were negligible in the spin-transfer measurements (Refs. [45,46] and Sec. III C), but that might cause systematic errors in the analyzing-power data.

1. Beam polarization + vs -

In Sec. III D we assumed that the spin flip was well behaved, so that the magnitude of P is the same for spin up and spin down. If, however, the polarization for spin up is $P + p$ and for spin down is $-P + p$, then A is given by

$$\frac{AP}{1+Ap} = \frac{r-1}{r+1}$$

and the correction $(1+Ap)$ needs to be considered. Measurements of P and p involve different techniques as follows.

The most precise polarization measurements [54] generally use a pair of detectors placed symmetrically to the left and right of the beam, measuring four cases: left L and right R with spin $+$ and $-$. In this case the correction term involving p cancels if N_+ is replaced by the geometric mean $\sqrt{N_{L+}N_{R-}}$ and similarly N_- by $\sqrt{N_{L-}N_{R+}}$. This technique is used with the beam line polarimeters to measure P , but not with the single-arm Vartola spectrometer.

Measurement of the difference term p requires separate measurements of the beam polarization $P+p$ for $+$ spin and $-P+p$ for $-$ spin. In principle, this can be obtained from the left-right ($L-R$) asymmetry in the polarimeters measured separately for each case, but then this must be corrected for the instrumental asymmetry Ω_R/Ω_L . Ω_R and Ω_L are the detector solid angles, or more strictly the products of the solid angles and efficiencies. Defining $r' = (N_L\Omega_R)/(N_R\Omega_L)$, then

$$A'(P+p) = \frac{r'-1}{r'+1}.$$

The ratio Ω_R/Ω_L was measured using unpolarized beam, obtained by blocking the OPPIS lasers (for 15 s) during the spin flip (every 2 min).

This measurement is subject to random noise from beam motion. (Beam motion is not correlated with the spin flip; see Sec. III E 3.) There are several ways to distinguish random noise from real effects, as follows.

First, a real difference should be observed in all polarimeters simultaneously. Second, instrumental asymmetries affect $+$ and $-$ spin oppositely and therefore leave the mean unchanged, whereas a short-term malfunction, e.g., affecting one spin state by 4%, would affect the mean by 2%. Third, a real short-term problem might be correlated with an identifiable malfunction. No cases were observed that satisfied two or more of these three criteria.

Long-term effects were examined by averaging over many independent readings. The average for all the data is $p = 0.000 \pm 0.001$, which is negligible. The average over the data at each angle gave values of $p = 0.01$ in nine cases, but none of these coincided with malfunctions that were expected to cause a real effect. In the worst case this would imply a correction of 0.001 to the final value of the analyzing power, which is negligible, and so in the final analysis it was assumed that the difference p was zero for all data.

2. Beam spot

On some occasions, differences of up to 3% have been observed between the polarization in the center and the fringes of the beam spot. This could cause a systematic error if the beam line polarimeters sampled the beam differently from the neutron production target. During

this experiment, however, the difference was small as a result of the moderate-sized aperture in OPPIS and the favorable tuning. Several different methods were used to check this variation, as follows.

A change in the quadrupole magnets changes the focus both on the beam line polarimeters and on the neutron production target. The resulting changes in the polarization were measured to be less than 1%.

When the spin-precession solenoid is turned off, the protons are left in the N -spin direction, which allows the two beam line polarimeters to give two independent measurements. Since these polarimeters are at two locations with different beam spot sizes, they have different sensitivity to the beam spot. Repeated tests compared the measurements with solenoids on and off in both polarimeters. Agreement was always better than 1%.

The LAMPF polarized beam is split between line B (where the present experiment was conducted) and the NTOF beam line by a pinhole stripper (LBST1), which directs the center of the beam spot to NTOF and the fringes to line B . NTOF took beam during some of the time at 635 MeV and most of the time at 485 MeV. During these periods the NTOF polarimeters were consistent with the line B polarimeters within 1%, confirming the uniformity of polarization across the beam spot.

Finally, we compared the analyzing power measured with only the fringes of the beam (when NTOF was taking the center) with the results obtained using the whole beam (when NTOF was off). The ratio was 1.002 ± 0.009 .

We therefore conclude that systematic errors from this possibility were less than 1%.

3. Beam stability

So far it has been assumed that Ω , t , and A (Sec. III D) are constant for the two spin states. Fluctuations in the beam spot could affect the detector solid angle Ω , effective target thickness t , or possibly the analyzing power A if the scattering angle changed. Random fluctuations introduce random noise into the data, which would cause internal inconsistency (from run to run; see Sec. III E 7), but average out over many runs. Fluctuations correlated with the spin flip are more serious and would introduce a systematic error.

The excellent characteristics of OPPIS are important in this respect. Spin flip is achieved by changing the frequency and polarization of the lasers, which have minimal effect on other beam parameters. We have examined these as follows.

The beam position and spot size at the neutron production target were read several times per second and the mean and standard deviations were recorded once per minute. Instability in the accelerator caused random fluctuations of about 1 mm, which is insignificant (see Sec. III E 7). Averaging these measurements at each angle, we measured the correlation with the spin flip to be less than 0.05 mm or 1% of the spot size. Beddo [55] has shown that this affects the asymmetry by less than 0.0001, which is negligible.

4. Beam intensity

Another important question concerns the stability of the beam intensity. Although we measure and correct for the incident beam for each state (I_+ and I_-), systematic errors could result from background or nonlinearity in the instruments if there were significant differences between the two states.

We monitored the beam intensities under a wide variety of conditions, throughout the analyzing power measurements as well as under extreme test conditions when the absorption of laser power in the OPPIS + and - states was very different. In all cases the average intensities in the + and - states agreed to within 0.1%.

Four detectors were used to measure the incident beam intensity: (1) a toroid between OPPIS and the LAMPF accelerator, (2) a toroid between the accelerator and the neutron production target, (3) a secondary emission monitor (SEM) placed 0.5 m upstream of the neutron production target, and (4) two pairs of scintillators viewing protons scattered up and down from the liquid hydrogen (LH_2) target. These monitors were compared with a clock in coincidence with the LAMPF beam gate to measure beam-on time.

The analyzing power was then calculated five ways: Each of the four beam monitors was used separately, and the clock was used in place of a beam monitor (which is equivalent to assuming constant beam intensity). These were found to be consistent within counting statistics. To test this we calculated the difference between each pair. At 635 and 788 MeV, the toroids agreed with the SEM with an average difference of 0.000 ± 0.001 (where 0.001 is the standard deviation of a single measurement from the mean). At 485 MeV, when the NTOF facility took a portion of the beam, the two toroids (which are upstream of the split) were not useful.

The two pairs of scintillators were limited by counting statistics, especially at some spectrometer settings when they had to be relegated to an unfavorable position far from the target. Although the standard deviation of a single measurement was typically 0.003, the overall mean (of the difference SEM minus scintillators) was 0.001 ± 0.001 , demonstrating the absence of systematic bias.

In summary, all the beam monitors were shown to be free of systematic errors, but the SEM had the smallest random error, and was therefore used in the final analysis.

5. Live time and efficiency

The measured numbers of events, N_+ and N_- , were corrected for detector efficiency and system live time.

The electronics and data-acquisition system was typically "live" (ready to accept an event) for 50%–90% of the time, depending on the event rate. The live time was measured in the standard manner by scaling event triggers with and without the electronic busy signal, and also by scaling a variety of beam-related signals with and without the busy signal in coincidence. This technique was examined during a recent absolute cross-section experiment [56] and shown to be accurate to 0.1%.

The detector efficiency could also be rate sensitive, and so this was measured by using redundant detectors to define a good event that should have registered in the detector of interest. The efficiency was then defined as the ratio of detected events to expected events. This technique was also examined in detail during the recent absolute cross-section experiment [56] and shown to be accurate to 0.2%. Efficiencies E were almost equal for the + and - spin states, with the correction factor E_+/E_- being typically about 0.998.

6. Electronic trigger

As in previous experiments [45,46,52] the standard electronic trigger included all scintillators in the magnetic spectrometer. It is conceivable that the presence of the carbon in the Janus polarimeter could cause a systematic error by scattering events away from the back scintillator. Such a systematic error would exist only if a large instrumental asymmetry in Janus [50] was combined with a large spin transfer so that the proton spin in Janus was correlated with the beam spin.

Rahbar [57] has shown that when the acceptance tests [58] are included, this possible error is eliminated. Nevertheless, to check this we compared data taken with and without the back scintillator in coincidence. In addition we analyzed all the data with and without the acceptance test [58]. In all cases the results were consistent within counting statistics.

7. Internal consistency

The experimental apparatus can introduce random noise into the data as a result of randomly changing conditions, but these were easily checked by examining internal consistency from one run to the next. A few percent of the runs were discarded because of known problems or malfunctions; almost all of these problems were associated with the 10 MHz beam bunching or rebunching systems. The remaining data were internally consistent within the counting statistics.

8. Rate tests

If the experimental apparatus was sensitive to the event rate, this could introduce a systematic error. Such a sensitivity might be associated with the live time or efficiency (Sec. III E 5) or some unidentified phenomenon.

To examine this we compared the analyzing power obtained from high-rate runs with low-rate runs taken at the same angles but with a factor-of-4 difference in the rates. In every case the data were consistent within counting statistics. Combining these, the difference (high rate minus low rate) was 0.0005 ± 0.0017 . We therefore conclude that this possible systematic error was also negligible.

9. Angles

The data were taken at 10 spectrometer-angle settings at 485 MeV and 11 settings at 635 and 788 MeV. The

settings were 5° apart in the laboratory, with each setting subdivided into three angle bins. A typical sequence of angle settings began with the even multiples of 5° , filled in with the odd multiples later so that slowly varying systematic errors might be apparent from discontinuities; none were observed.

Although the absolute angles were surveyed to better than 0.1° laboratory (0.2° c.m.), an independent check is important. The precise data near 70° c.m. from TRIUMF [36] determined the zero-crossing angle to be 70.01° with a statistical uncertainty of 0.07° and an estimated systematic uncertainty of 0.1° . This agrees well with the fit to our 485 MeV data, where the zero-crossing angle was 69.95° with a statistical uncertainty of 0.10° .

10. Summary of systematic errors

Although we have confirmed that each individual systematic error is small, it does not follow that the quadratic sum of all systematic errors is negligible. We summarize the upper limits on each possible error in this section.

Some uncertainties are additive (e.g., ± 0.003) and some are multiplicative (e.g., 1%). A 1% multiplicative error corresponds to ± 0.003 when applied to a data value of 0.3.

The uncertainty in the neutron-beam polarization contributes an overall normalization uncertainty of 2% (2.4% at 788 MeV) to all angles at a single energy, as stated in Sec. III C. In addition, there is a point-to-point uncertainty (Sec. III E 2) of 1% or less.

The uncertainty in absolute angle contributes 0.003 where the slope is steep near 70° and zero near 110° . Note that the uncertainty from beam polarization is large (1% of 0.3) when the uncertainty in angle is small and vice versa so that the combined uncertainty is about 0.003 at most angles.

Note also that an uncertainty of 0.2% in the efficiency contributes close to 0.002 to the analyzing power (since P is about 0.5 and $r + 1$ is about 2).

In summary the following points can be made: (i) beam polarization, overall (Sec. III C): 2% or 2.4%; (ii) beam polarization, point to point (Sec. III E 2): 0–0.003; (iii) absolute angle (Sec. III E 9): 0–0.003; (iv) beam intensity (Sec. III E 4): 0.001; (v) efficiency (Sec. III E 5): 0.002; (vi) total point-to-point systematic uncertainty: 0.003–0.004; (vii) overall normalization uncertainty: 2% or 2.4%.

This estimate has been combined (quadratically) with the statistical uncertainties (typically 0.003–0.005) to give the overall point-to-point uncertainty in the tables.

IV. RENORMALIZATION OF PREVIOUS DATA

Neutron-beam polarization was recently recalibrated by double scattering [19]. The results disagreed with the older calibration [59,60], which was based on the measurement by Newsom *et al.* [38] of the np -elastic analyzing power. Section IV of Ref. [19] lists six reasons that support the newer [19] versus the older [59,60] calibration, and suggested that the calibration of the

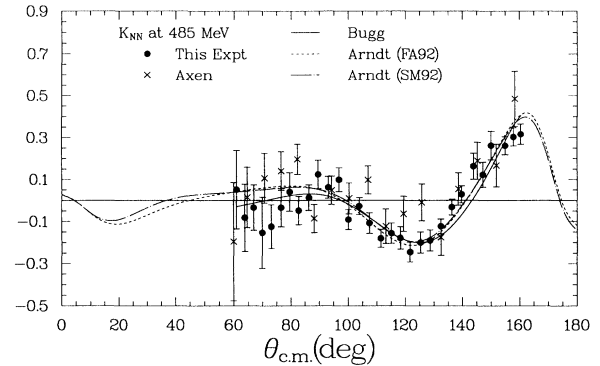


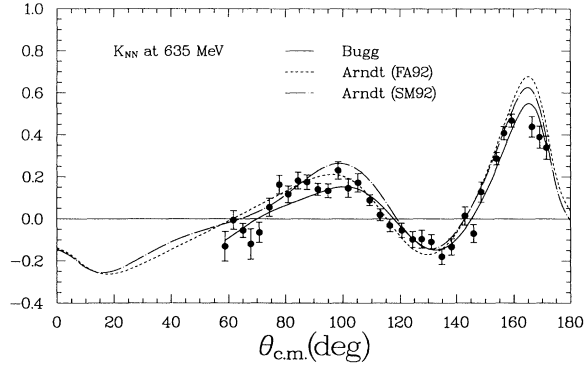
FIG. 1. K_{NN} at 485 MeV. The SM92 analysis of Arndt *et al.* precedes our data. The FA92 fit of Arndt *et al.* and Bugg's fit include our data.

polarized-proton target may have been incorrect, leading to an incorrect normalization of the analyzing-power data. The present remeasurement of the analyzing power adds weight to that conclusion.

The data of Newsom *et al.* [38] are consistently larger in magnitude than the data reported here. The

TABLE I. K_{NN} for ${}^1\text{H}(n,n)p$ at 485 MeV. The overall normalization uncertainty is 2.0% (see Sec. III C). The angle is the neutron c.m. angle (degrees); i.e., 180° represents a backward neutron and forward proton.

$\theta_{\text{c.m.}}$ (deg)	K_{NN}
160.45	0.316 ± 0.049
157.84	0.303 ± 0.043
154.93	0.261 ± 0.043
150.05	0.262 ± 0.068
147.14	0.123 ± 0.060
143.85	0.163 ± 0.062
139.71	0.029 ± 0.041
136.34	-0.032 ± 0.038
132.51	-0.123 ± 0.035
128.66	-0.190 ± 0.050
125.31	-0.200 ± 0.050
121.71	-0.245 ± 0.047
118.26	-0.179 ± 0.053
115.15	-0.156 ± 0.048
111.39	-0.180 ± 0.043
107.46	-0.108 ± 0.049
103.89	-0.027 ± 0.041
100.14	-0.091 ± 0.047
96.82	0.099 ± 0.057
93.12	0.062 ± 0.052
89.57	0.124 ± 0.068
86.34	0.013 ± 0.061
82.79	-0.048 ± 0.067
79.55	0.041 ± 0.092
76.62	-0.034 ± 0.091
73.12	-0.124 ± 0.104
69.92	-0.153 ± 0.169
66.88	-0.034 ± 0.108
63.81	-0.082 ± 0.160
60.87	0.052 ± 0.187

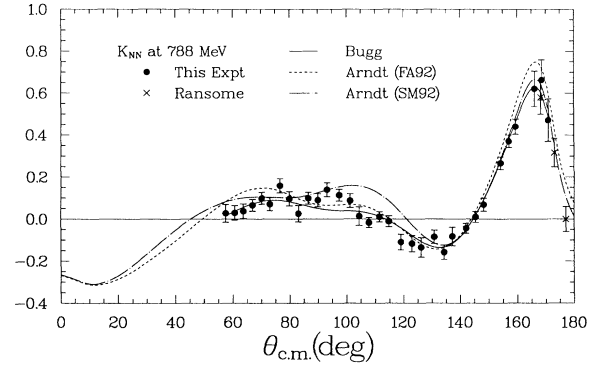
FIG. 2. K_{NN} at 635 MeV. The fits are as for Fig. 1.

best agreement is obtained by multiplying the values of Newsom *et al.* by 0.90, 0.88, and 0.86 near 500, 650, and 800 MeV, respectively. The corresponding ratios of the neutron-beam calibrations (old/new) are 0.86 ± 0.03 , 0.93 ± 0.03 , and 0.84 ± 0.04 . These are consistent with a single renormalization factor of 0.88.

It has been suggested that the 3.8-cm lead plug that

TABLE II. K_{NN} for $^1\text{H}(n,n)p$ at 635 MeV. The overall normalization uncertainty is 2.0% (see Sec. III C).

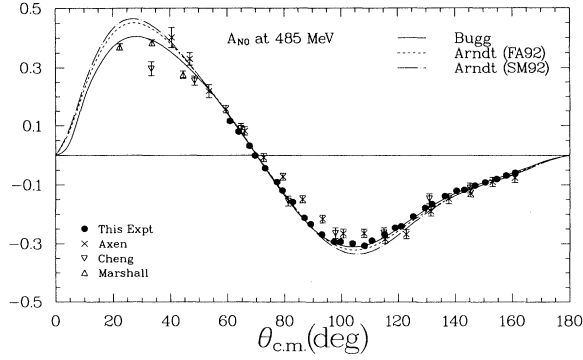
$\theta_{c.m.}$ (deg)	K_{NN}
171.54	0.339 ± 0.055
169.13	0.389 ± 0.053
166.42	0.439 ± 0.049
159.26	0.468 ± 0.031
156.69	0.408 ± 0.031
153.99	0.287 ± 0.029
148.59	0.128 ± 0.048
145.94	-0.070 ± 0.043
142.98	0.014 ± 0.043
138.31	-0.133 ± 0.039
134.93	-0.180 ± 0.037
131.13	-0.110 ± 0.035
127.69	-0.097 ± 0.043
124.45	-0.098 ± 0.038
120.55	-0.054 ± 0.034
116.41	-0.031 ± 0.030
113.03	0.019 ± 0.028
109.38	0.089 ± 0.026
105.28	0.172 ± 0.044
101.90	0.146 ± 0.044
98.44	0.231 ± 0.042
94.96	0.134 ± 0.033
91.40	0.141 ± 0.029
87.60	0.175 ± 0.035
84.44	0.182 ± 0.040
81.03	0.117 ± 0.040
77.82	0.163 ± 0.045
74.35	0.055 ± 0.043
70.78	-0.065 ± 0.048
67.78	-0.120 ± 0.073
65.04	-0.055 ± 0.034
61.73	-0.006 ± 0.044
58.81	-0.131 ± 0.071

FIG. 3. K_{NN} at 788 MeV. The fits are as for Fig. 1.

was used to attenuate the gamma rays in previous experiments may have affected the neutron-beam polarization. We checked this possibility by measuring the np analyzing power with and without a 5.1-cm lead plug in the neutron beam. The ratio of the measurements with or without the plug was 0.994 ± 0.011 . This demonstrates that the effect of the 3.8-cm plug was negligible.

TABLE III. K_{NN} for $^1\text{H}(n,n)p$ at 788 MeV. The overall normalization uncertainty is 2.4% (see Sec. III C).

$\theta_{c.m.}$ (deg)	K_{NN}
170.97	0.471 ± 0.101
168.67	0.663 ± 0.096
166.13	0.621 ± 0.085
159.40	0.440 ± 0.036
157.05	0.370 ± 0.030
154.18	0.266 ± 0.030
148.27	0.068 ± 0.031
145.47	0.010 ± 0.026
142.11	-0.044 ± 0.024
137.21	-0.083 ± 0.044
134.36	-0.158 ± 0.034
130.84	-0.085 ± 0.032
126.25	-0.135 ± 0.046
123.06	-0.117 ± 0.039
119.10	-0.110 ± 0.037
114.89	-0.011 ± 0.026
111.56	0.011 ± 0.024
107.88	-0.017 ± 0.024
104.49	0.014 ± 0.044
101.30	0.087 ± 0.033
97.50	0.113 ± 0.028
93.23	0.139 ± 0.033
89.99	0.089 ± 0.031
86.63	0.098 ± 0.028
83.17	0.026 ± 0.039
79.97	0.096 ± 0.034
76.62	0.158 ± 0.034
73.07	0.070 ± 0.031
70.17	0.098 ± 0.028
66.94	0.065 ± 0.028
63.75	0.037 ± 0.034
60.73	0.029 ± 0.034
57.55	0.027 ± 0.042

FIG. 4. A_{N0} at 485 MeV. The fits are as for Fig. 1.

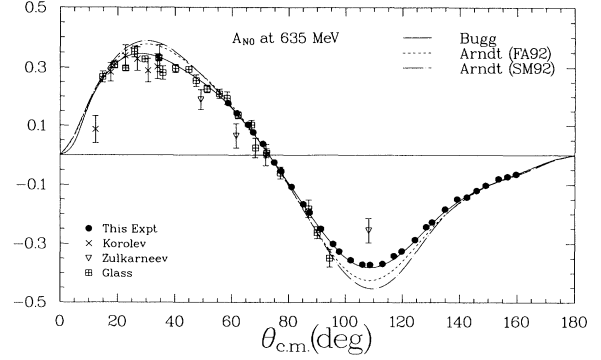
We conclude that the previous np -elastic measurements that used the LAMPF polarized-neutron beam should be renormalized as suggested in Sec. V of Ref. [19].

V. CONCLUSION

Data are listed in Tables I–VI and shown in Figs. 1–6 in comparison with previous data and the most recent phase-shift fits, which include these data. Previous

TABLE IV. A_{N0} for ${}^1\text{H}(n,n)p$ at 485 MeV. The overall normalization uncertainty is 2.0% (see Sec. III C).

$\theta_{c.m.}$ (deg)	A_{N0}
160.99	-0.059 ± 0.004
157.84	-0.068 ± 0.004
154.53	-0.080 ± 0.004
150.54	-0.091 ± 0.005
146.92	-0.102 ± 0.005
143.17	-0.117 ± 0.005
140.45	-0.120 ± 0.004
136.34	-0.138 ± 0.004
131.82	-0.165 ± 0.004
129.42	-0.178 ± 0.004
125.31	-0.208 ± 0.004
121.09	-0.241 ± 0.004
118.94	-0.246 ± 0.005
115.15	-0.268 ± 0.005
110.74	-0.289 ± 0.005
108.10	-0.305 ± 0.006
103.89	-0.300 ± 0.006
99.66	-0.293 ± 0.006
97.49	-0.293 ± 0.005
93.12	-0.268 ± 0.005
89.20	-0.233 ± 0.005
87.00	-0.212 ± 0.006
82.79	-0.158 ± 0.006
79.19	-0.119 ± 0.006
77.29	-0.091 ± 0.005
73.12	-0.042 ± 0.005
69.65	0.000 ± 0.005
67.63	0.032 ± 0.005
63.90	0.080 ± 0.005
60.84	0.116 ± 0.005

FIG. 5. A_{N0} at 635 MeV. The fits are as for Fig. 1.

data with uncertainties greater than 10 times those of the present data are not shown. Apart from the exceptions discussed in Sec. II, agreement is generally satisfactory.

With the inclusion of the present data the single-energy phase-shift analyses (PSA) of Arndt *et al.* [3] and Bugg and Bryant [4,7] are now well determined at 500, 650, and 800 MeV, with good χ^2 minima and small correlation coefficients. The single-energy fit of Arndt *et al.* (C800) now agrees with that of Bugg and Bryan to about

TABLE V. A_{N0} for ${}^1\text{H}(n,n)p$ at 635 MeV. The overall normalization uncertainty is 2.0% (see Sec. III C).

$\theta_{c.m.}$ (deg)	A_{N0}
159.67	-0.064 ± 0.005
156.69	-0.072 ± 0.005
153.56	-0.080 ± 0.005
149.11	-0.102 ± 0.005
145.94	-0.121 ± 0.005
142.55	-0.141 ± 0.005
139.11	-0.150 ± 0.005
134.93	-0.183 ± 0.005
130.43	-0.228 ± 0.005
128.37	-0.246 ± 0.005
124.45	-0.285 ± 0.005
119.81	-0.325 ± 0.005
117.11	-0.341 ± 0.005
113.05	-0.368 ± 0.005
108.70	-0.371 ± 0.005
106.02	-0.370 ± 0.005
101.90	-0.355 ± 0.005
97.82	-0.326 ± 0.005
95.66	-0.301 ± 0.004
91.40	-0.250 ± 0.004
87.46	-0.195 ± 0.004
85.12	-0.166 ± 0.005
81.03	-0.107 ± 0.005
77.43	-0.054 ± 0.005
74.99	-0.025 ± 0.005
70.87	0.038 ± 0.005
67.49	0.077 ± 0.005
65.66	0.103 ± 0.004
61.73	0.143 ± 0.004
58.60	0.177 ± 0.004

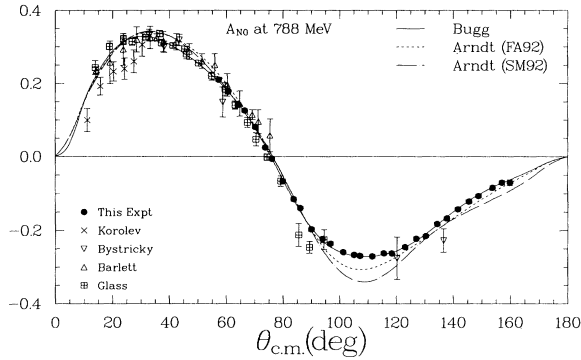


FIG. 6. A_{N0} at 788 MeV. The fits are as for Fig. 1.

a degree for all real isospin-0 phases.

The energy-dependent fit (FA92), however, diverges from the single-energy fits above 500 MeV. At 800 MeV the 1P_1 phases disagree by 7° and 3D_2 by 4° . This may result from inadequate data at energies above 800 MeV, which influence the 800 MeV solutions by constraining the phases to follow smooth curves. Despite extensive data, two weaknesses in the data still allow this flexibility.

First, most PSA's renormalize individual data sets at the cost of a small χ^2 penalty, for example, Arndt *et al.*, Bugg and Bryan, and the Saclay group renormalize the data of Korolev *et al.* [32] by 10%, 20%, and 0%, respectively. Cross calibration would help to tie together the normalization of different data sets. For example, by extending our analyzing-power measurements to forward angles, we could tie together the normalization of the forward- and backward-angle peaks and also tie the np to the pp normalization via the quasifree measurements that used the polarized-proton beam on a deuterium target [28,31].

The second weakness is with the inelasticities. Each PSA fits isospin-0 inelasticity to different partial waves: Arndt *et al.* choose 3S_1 , 3D_1 , 3D_3 , 1F_3 , 3G_3 , and 1H_5 ; Bugg and Bryan choose 1P_1 , 3D_1 , 3D_3 , and 3G_3 ; Hoshizaki and Watanabe [6] choose 3S_1 , 1P_1 , 3D_1 , 3D_2 , and 3D_3 ; while the Saclay group confines inelasticity to 3D_1 and 3D_2 . Bugg [7] points out that the real parts of the phase shifts contain clues to the inelasticities, but these require accurate determination of the higher partial waves where agreement among the PSA's is inadequate. The analyzing-power data are a sensitive probe of these waves; this provides another motive for extending these precise measurements to forward angles.

The mixing parameter ϵ_1 is sensitive to K_{NN} . It is gratifying that with these new data the predictions of Arndt *et al.* and Bugg and Bryan for ϵ_1 are converging, and are in reasonable agreement with Lomon's calcula-

TABLE VI. A_{N0} for $^1H(n,n)p$ at 788 MeV. The overall normalization uncertainty is 2.4% (see Sec. III C).

$\theta_{c.m.}$ (deg)	A_{N0}
159.90	-0.070 ± 0.008
157.05	-0.070 ± 0.006
153.80	-0.084 ± 0.005
148.82	-0.106 ± 0.004
145.47	-0.121 ± 0.004
141.60	-0.142 ± 0.004
137.78	-0.167 ± 0.005
134.36	-0.183 ± 0.005
130.32	-0.214 ± 0.005
126.99	-0.222 ± 0.005
123.06	-0.245 ± 0.005
118.42	-0.262 ± 0.005
115.58	-0.262 ± 0.004
111.46	-0.270 ± 0.004
107.14	-0.269 ± 0.004
105.10	-0.265 ± 0.005
101.30	-0.258 ± 0.005
96.76	-0.238 ± 0.005
93.93	-0.224 ± 0.005
89.99	-0.195 ± 0.005
86.08	-0.140 ± 0.005
83.79	-0.118 ± 0.005
79.97	-0.064 ± 0.005
76.10	-0.006 ± 0.005
73.75	0.024 ± 0.005
70.17	0.081 ± 0.005
66.52	0.126 ± 0.005
64.20	0.142 ± 0.005
60.73	0.178 ± 0.005
57.31	0.209 ± 0.005

tions [61].

In conclusion, our measurements of A_{N0} for np -elastic scattering are a factor of 10 better than previous measurements, and clarify the renormalization problem, which affects previous LAMPF data. Our K_{NN} data are unique near 800 MeV, replace incorrect data near 650 MeV, and agree with less precise data near 500 MeV. These new data complete the set needed to extract the nucleon-nucleon scattering amplitudes near 500, 650, and 800 MeV.

ACKNOWLEDGMENTS

This work is supported in part by U.S. Department of Energy Contracts Nos. W-7405-ENG-36 and W-31-109-ENG-38, by Grants Nos. DE-FG05-88ER40446 and DE-FG05-88ER40399, and by the National Science Foundation.

- [1] M.W. McNaughton *et al.*, Phys. Rev. C **41**, 2809 (1990).
 [2] G. Glass *et al.*, Phys. Rev. C **45**, 35 (1992).
 [3] R.A. Arndt *et al.*, Phys. Rev. D **45**, 3995 (1992).
 [4] D.V. Bugg, Phys. Rev. C **41**, 2708 (1990).

- [5] J. Bystricky, C. Leluc, and F. Lehar, J. Phys. (Paris) **48**, 199 (1987).
 [6] N. Hoshizaki and T. Watanabe, Prog. Theor. Phys. **86**, 321 (1991).

- [7] D.V. Bugg and R.A. Bryan, Nucl. Phys. **A540**, 449 (1992).
- [8] M.W. McNaughton, R.R. Silbar, and O.B. van Dyck, Los Alamos Report No. LA-10051-MS, 1984.
- [9] J. Bystricky, F. Lehar, and P. Winternitz, J. Phys. (Paris) **39**, 1 (1978).
- [10] *Higher Energy Polarized Beams (Ann Arbor, 1977)*, Proceedings of the Workshop on Higher Energy Polarized Proton Beams, edited by A.D. Krisch and A.J. Salthouse, AIP Conf. Proc. No. 42 (AIP, New York, 1978), p. 142.
- [11] P. Lisowski *et al.*, Phys. Rev. Lett. **49**, 255 (1982).
- [12] T.J. Devlin *et al.*, Phys. Rev. D **8**, 136 (1973).
- [13] V. Grundies *et al.*, Phys. Lett. **158B**, 15 (1985).
- [14] R.K. Keeler *et al.*, Nucl. Phys. **A377**, 529 (1982).
- [15] I.P. Auer *et al.*, Phys. Rev. Lett. **46**, 1177 (1981).
- [16] M.E. Beddo *et al.*, Phys. Lett. B **258**, 24 (1991).
- [17] Y. Terrien *et al.*, Nucl. Phys. **A478**, 533 (1988).
- [18] R. Binz *et al.*, Nucl. Phys. **A533**, 601 (1991).
- [19] M.W. McNaughton *et al.*, Phys. Rev. C **45**, 2564 (1992).
- [20] R. Carlini *et al.*, Phys. Rev. Lett. **41**, 1341 (1978).
- [21] B.E. Bonner *et al.*, Phys. Rev. Lett. **41**, 1200 (1978).
- [22] M. Evans *et al.*, Phys. Rev. C **26**, 2525 (1982).
- [23] L.C. Northcliffe *et al.*, Phys. Rev. C **47**, 36 (1993).
- [24] M. Jain *et al.*, Phys. Rev. Lett. **30**, 566 (1984).
- [25] Y. Terrien *et al.*, Phys. Rev. Lett. **59**, 1534 (1987).
- [26] D. Cheng *et al.*, Phys. Rev. **163**, 1470 (1967).
- [27] R. Zulkarneev *et al.*, Phys. Lett. **61B**, 164 (1976).
- [28] M.L. Barlett *et al.*, Phys. Rev. C **27**, 682 (1983).
- [29] J.A. Marshall *et al.*, Phys. Rev. C **34**, 1433 (1986).
- [30] J. Bystricky *et al.*, Nucl. Phys. **A444**, 597 (1985).
- [31] G. Glass *et al.*, Phys. Rev. C **47**, 1369 (1993).
- [32] G.A. Korolev *et al.*, Phys. Lett. **165B**, 262 (1985).
- [33] G. Glass *et al.*, Phys. Rev. C **41**, 2732 (1990).
- [34] B.H. Silverman *et al.*, Nucl. Phys. **A499**, 763 (1989).
- [35] A.S. Clough *et al.*, Phys. Rev. C **21**, 988 (1980).
- [36] D. Bandyopadhyay *et al.*, Phys. Rev. C **40**, 2684 (1989).
- [37] A. De Lesquen *et al.*, Nucl. Phys. **B304**, 673 (1988).
- [38] C.R. Newsom *et al.*, Phys. Rev. C **39**, 965 (1989).
- [39] W.R. Ditzler *et al.*, Phys. Rev. D **46**, 2792 (1992).
- [40] T. Shima *et al.*, Phys. Rev. D **47**, 29 (1993).
- [41] J. Ball *et al.*, Z. Phys. C **40**, 193 (1988).
- [42] M.L. Barlett *et al.*, Phys. Rev. C **32**, 239 (1985).
- [43] M.L. Barlett *et al.*, Phys. Rev. C **40**, 2697 (1989).
- [44] D. Axen *et al.*, Phys. Rev. C **21**, 998 (1980).
- [45] M.W. McNaughton *et al.*, Phys. Rev. C **44**, 2267 (1991).
- [46] K.H. McNaughton *et al.*, Phys. Rev. C **46**, 47 (1992).
- [47] R.D. Ransome *et al.*, Phys. Rev. Lett. **48**, 781 (1982).
- [48] P.H. Surko, University of California Report No. UCRL-19451, 1970.
- [49] M.W. McNaughton and E.P. Chamberlin, Phys. Rev. C **24**, 1778 (1981).
- [50] R.A. Ransome *et al.*, Nucl. Instrum. Methods **201**, 309 (1982).
- [51] R. Garnett *et al.*, Nucl. Instrum. Methods A **309**, 508 (1991).
- [52] M.W. McNaughton *et al.*, Phys. Rev. C **25**, 1967 (1982).
- [53] M.W. McNaughton *et al.*, Nucl. Instrum. Methods A **241**, 435 (1985).
- [54] G.G. Ohlsen and P.W. Keaton, Nucl. Instrum. Methods **109**, 41 (1973).
- [55] M.E. Beddo, Ph.D. thesis, New Mexico State University, 1990; Los Alamos Report No. LA-11905-T, 1990.
- [56] A.J. Simon *et al.*, Phys. Rev. C (to be published).
- [57] A. Rahbar, Ph.D. thesis, University of California, Los Angeles, 1982; Los Alamos Report No. LA-9505-T, 1982.
- [58] D. Besset *et al.*, Nucl. Instrum. Methods **166**, 515 (1979).
- [59] P.J. Riley *et al.*, Phys. Lett. **103B**, 313 (1981).
- [60] J.S. Chalmers *et al.*, Phys. Lett. **153B**, 235 (1985).
- [61] E.L. Lomon, Phys. Rev. D **26**, 576 (1982).